Supporting Information

# Role of Plasticity in Mechanical Failure of Solid Electrolyte Interphases on Nanostructured Silicon Electrode: Insight from Continuum Level Modeling.

Masatomo Tanaka[1], Justin B. Hooper[2], Dmitry Bedrov[2,*]

[1] Murata Manufacturing Co., Ltd., 1-10-1 Higashikotari, Nagaokakyo-shi, Kyoto 617-8555, Japan

[2] Department of Materials Science & Engineering University of Utah, 122 S. Central Campus Dr., Salt Lake City, UT 84109, USA.

* Corresponding author: d.bedrov@utah.edu

*The change in void volume fraction*

The voids evolve through growth and nucleation, while the void evolution, growth and nucleation rates of the voids are respectively calculated as

$$\dot{f} = \dot{f}_{nucl} + \dot{f}_{grow} \tag{S1}$$

$$\dot{f}_{grow} = (1 - f)\mathrm{Tr}\left(\boldsymbol{D_p}\right) \tag{S2}$$

$$\dot{f}_{nucl} = \frac{f_n}{(s_n\sqrt{2\pi})} exp\left[-\frac{1}{2}\frac{(\epsilon_p - \epsilon_n)^2}{s_n^2}\right]\dot{\epsilon_p}, \tag{S3}$$

where $\boldsymbol{D_p}$ is the time derivative of the plastic deformation tensor, $f_n$ is the volume fraction of the void-nucleating particles, $\epsilon_p$ and $\dot{\epsilon_p}$ denote the plastic strain and its rate, respectively, and $\epsilon_n$ and $s_n$ are the mean and standard deviation of the nucleation strain distribution, respectively. Here we assumed the typical values for ductile materials: $f_n = 0.1$, $\epsilon_n = 0.3$, $s_n = 0.1$ and critical porosity $f_c = 0.3$.

*Computational environment*

The simulation was performed on 9 cores of a single computer node with an Intel Xeon E5-2667 CPU at a clock speed of 2.90 GHz. The simulation was completed after 99,399 time steps, requiring ~88.35 h (estimated from a wall clock).

*The effect of failure stress for $Li_2CO_3$ SEI layer in the brittle-fracture model*

**Figure S1** shows the evolving failure in the $Li_2CO_3$ SEI layer in the brittle-fracture model. **Table S1** lists the values of the mechanical properties. Under high failure stress, the SEI failure again initiated from the corner of the silicon nanopillar.

**Table S1**. *Mechanical properties in the brittle fracture model.*

| | Bulk modulus (GPa) | Shear modulus (GPa) | Yield stress (GPa) | Work hardening modulus (GPa) | Failure stress (MPa) | Reference number |
|---|---|---|---|---|---|---|
| $Li_2CO_3$ - SI -1 | 50.5 | 22.2 | - | - | 1000 | 22, 23 |
| $Li_2CO_3$ - SI -3 | 50.5 | 22.2 | - | - | 2000 | 22, 23 |
| $Li_2CO_3$ - SI -3 | 50.5 | 22.2 | - | - | 3000 | 22, 23 |

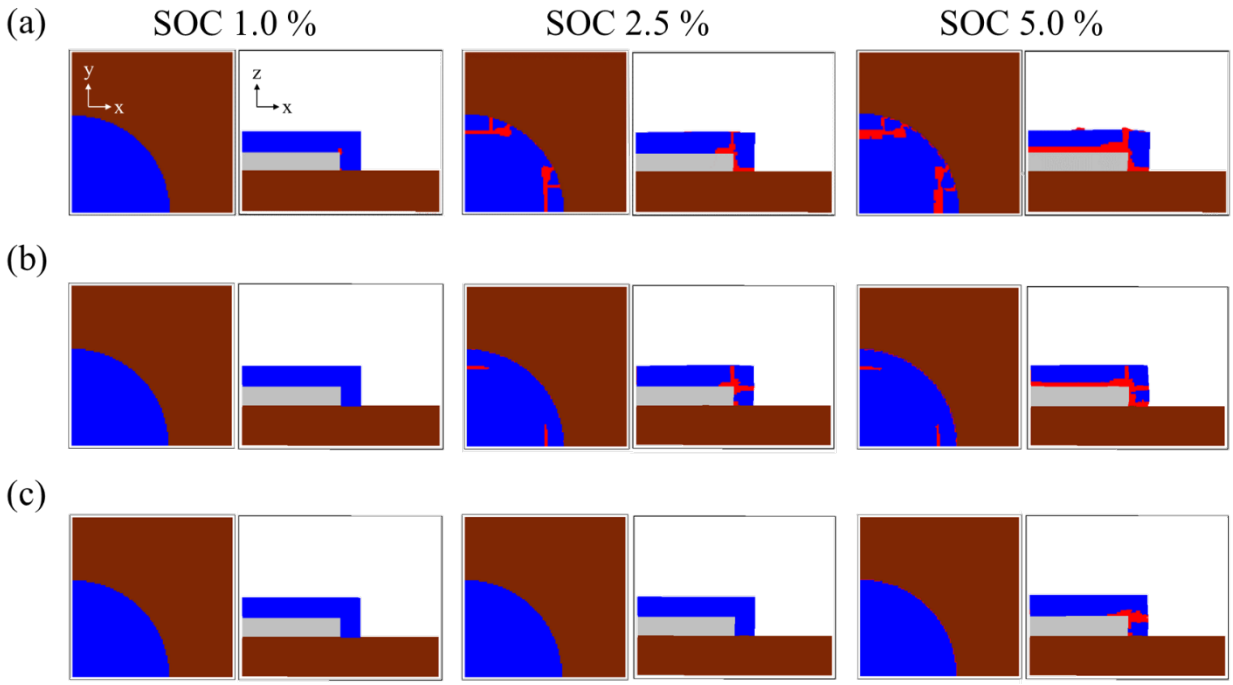


**Figure S1.** *Failure evolution of the $Li_2CO_3$ SEI layer in the brittle fracture model under high failure stress at differing SOCs. Each panel displays an overhead view (left) and a side view (right). Red and blue regions highlight the failure and non-failure regions in the SEI layer, respectively. (a) $Li_2CO_3$ – SI – 1 (1,000 MPa), (b) $Li_2CO_3$ – SI – 2 (2,000 MPa) and (c) $Li_2CO_3$ – SI – 3 (3,000 MPa).*

*The effect of failure-stress distribution for $Li_2CO_3$ SEI layer in the brittle-fracture model*

By examining the failure-stress distribution in the SEI, we can examine the impact of irregular composition on the failure mode. The probability density distribution of the failure stress is assumed to be Gaussian. The Gaussian distribution is given by

$$f(x) = \frac{1}{\sqrt{2\pi}\sigma} exp\left(-\frac{(x-\mu)^2}{2\sigma^2}\right), \quad \text{(S4)}$$

where $\mu$ and $\sigma$ are the mean and standard deviation of the distribution, respectively. **Figures S2** and **S3** show the failure-stress distributions and evolution in the $Li_2CO_3$ SEI layer, respectively. As observed in the uniform model, SEI failure in the failure-stress distribution model proceeded from the corner of the silicon nanopillar.

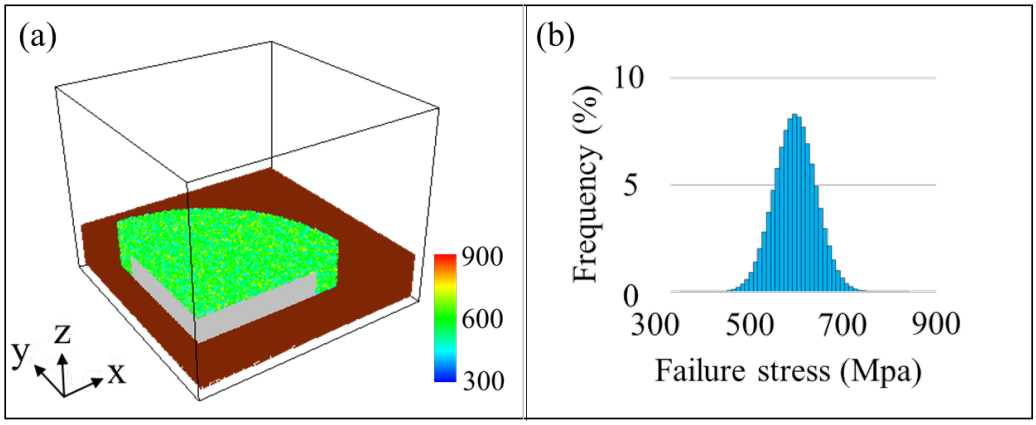


**Figure S2.** *Failure-stress distribution in the $Li_2CO_3$ SEI layer with $\mu$ = 581 MPa, $\sigma$ = 48 MPa. (a) Failure-stress contours and (b) failure-stress histogram in the $Li_2CO_3$ layer.*

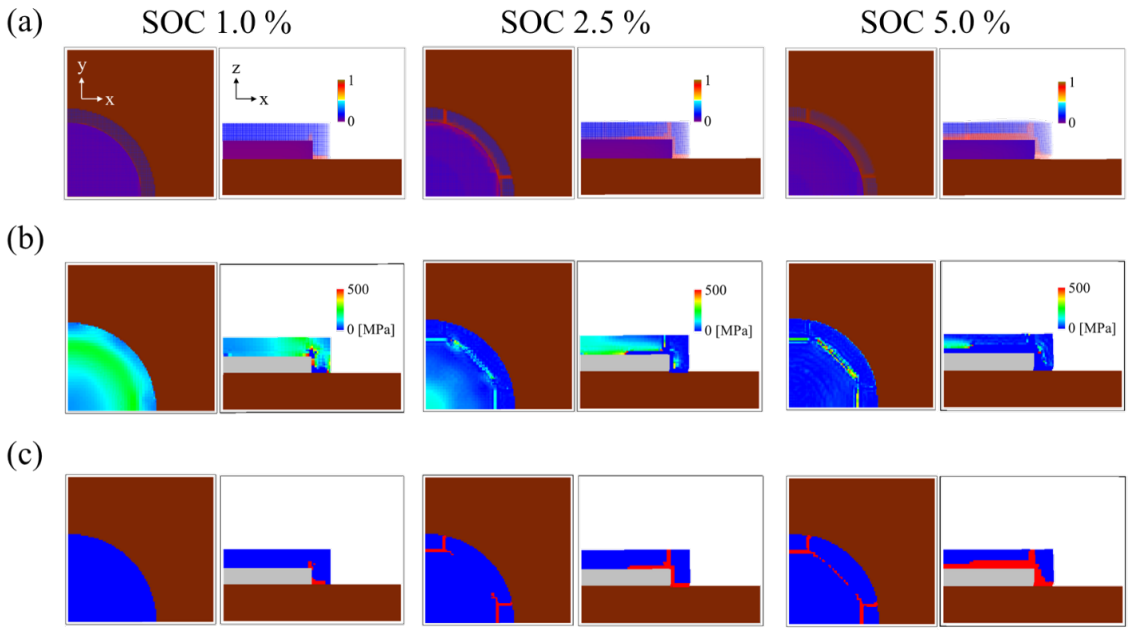


**Figure S3.** *Lithium concentration of silicon nanopillar, stress and failure evolution of the $Li_2CO_3$ SEI layer during lithiation in the brittle fracture model with stress distribution at differing SOCs. Each panel displays an overhead view (left) and a side view (right). (a) lithium concentration of silicon, (b) maximum principal stress of the $Li_2CO_3$ SEI layer, and (c) failure location of the $Li_2CO_3$*

*SEI layer. Red and blue regions indicate the failure and non-failure regions in the SEI layer, respectively.*

*The elastic-brittle PEO model*

**Figure S4** shows the failure evolution of the PEO SEI layer in the brittle fracture model, assuming the mechanical properties of PEO. **Table S1** lists the values of the mechanical properties. The SEI initially failed at the corner of the silicon nanopillar.

**Table S2**. *Mechanical properties in the brittle fracture model for PEO SEI layer.*

| | Bulk modulus (GPa) | Shear modulus (GPa) | Yield stress (GPa) | Work hardening modulus (GPa) | Failure stress (MPa) | Reference number |
|---|---|---|---|---|---|---|
| PEO - SI -1 | 2.4 | 0.89 | - | - | 70 | 22, 23 |

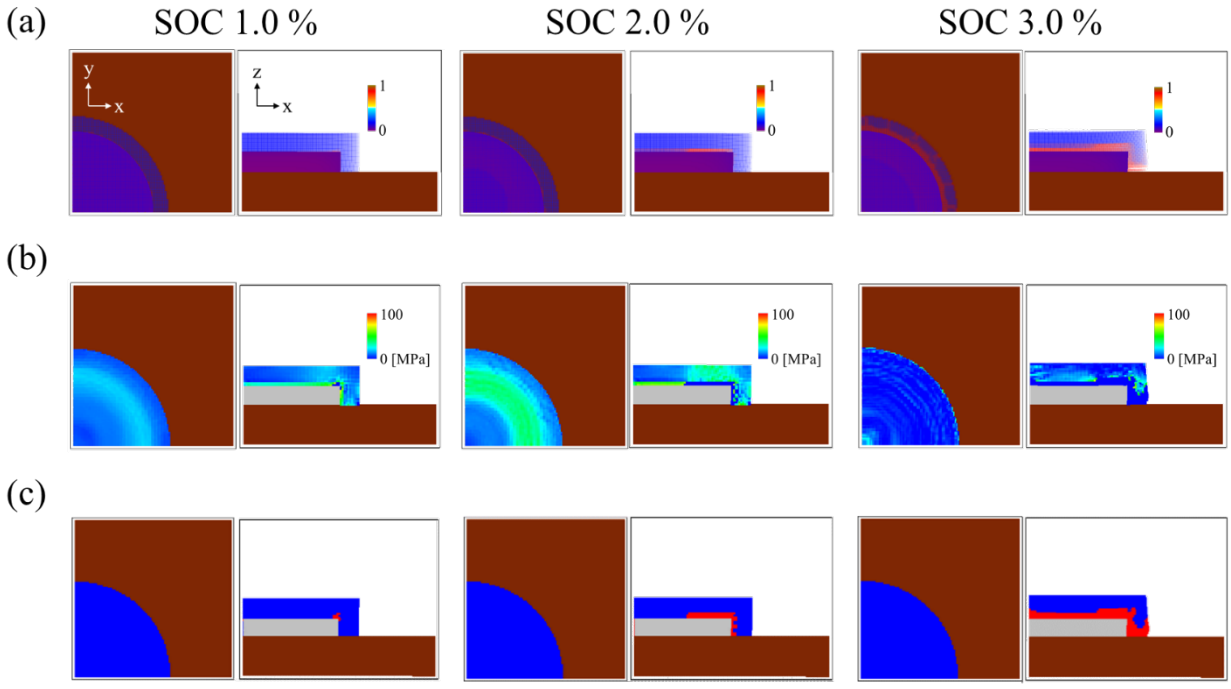


**Figure S4.** *Lithium concentration of silicon nanopillar, stress and failure evolution of the PEO SEI layer during lithiation in the brittle fracture model at differing SOCs. Each panel displays an overhead view (left) and a side view (right). (a) lithium concentration of silicon, (b) maximum principal stress of the PEO SEI layer, and (c) failure location of the PEO SEI layer. Red and blue regions indicate the failure and non-failure regions in the SEI layer, respectively.*

*The effect of failure stress for PEO SEI layer in the brittle-fracture model*

**Figure S5** shows the evolving failure in the PEO SEI layer in the brittle-fracture model. **Table S3** lists the values of the mechanical properties. Under high failure stress, the SEI failure again initiated from the corner of the silicon nanopillar.

**Table S3**. *Mechanical properties in the brittle fracture model.*

| | Bulk modulus (GPa) | Shear modulus (GPa) | Yield stress (GPa) | Work hardening modulus (GPa) | Failure stress (MPa) | Reference number |
|---|---|---|---|---|---|---|
| PEO - SI -2 | 2.4 | 0.89 | - | - | 140 | 22, 23 |
| PEO - SI -3 | 2.4 | 0.89 | - | - | 210 | 22, 23 |
| PEO - SI -4 | 2.4 | 0.89 | - | - | 300 | 22, 23 |

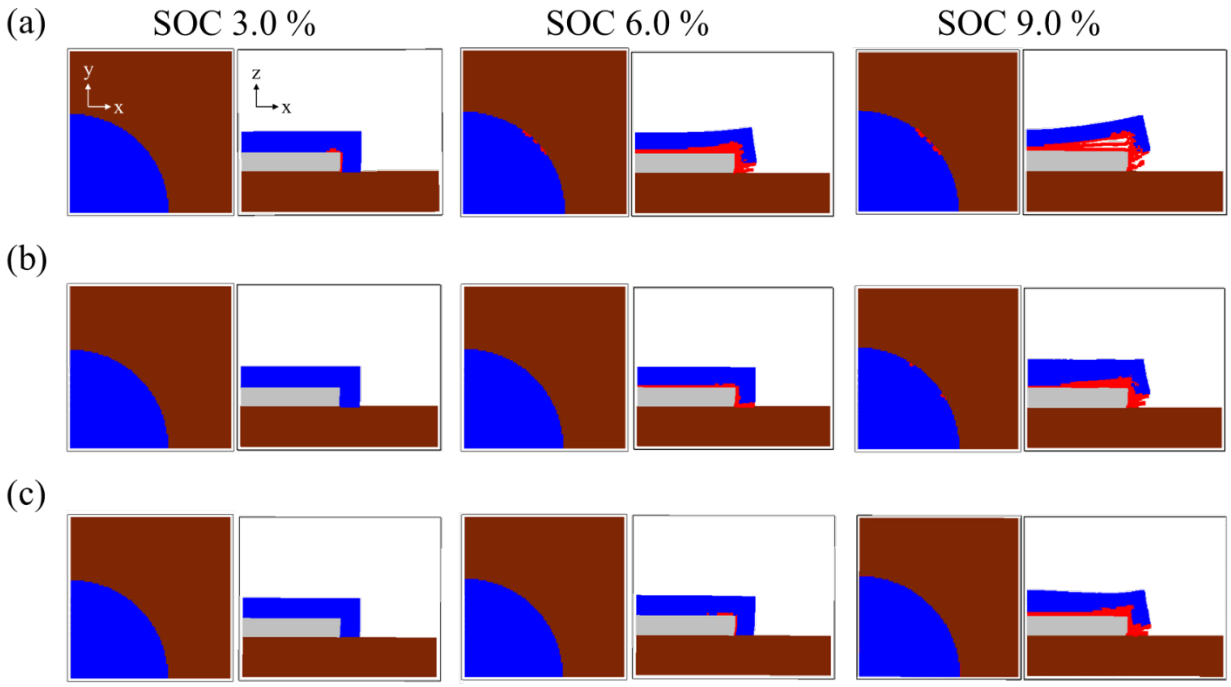


**Figure S5.** *Failure evolution of the PEO SEI layer in the brittle fracture model under high failure stress at differing SOCs. Each panel displays an overhead view (left) and a side view (right). Red and blue regions highlight the failure and non-failure regions in the SEI layer, respectively. (a) PEO – SI – 2 (140 MPa), (b) PEO – SI – 3 (210 MPa) and (c) PEO – SI – 3 (300 MPa).*

*The effect of failure-stress distribution for PEO SEI layer in the brittle-fracture model*

**Figures S6** and **S7** show the failure-stress distributions and evolution in the PEO SEI layer, respectively. As observed in the uniform model, SEI failure in the failure-stress distribution model proceeded from the corner of the silicon nanopillar.

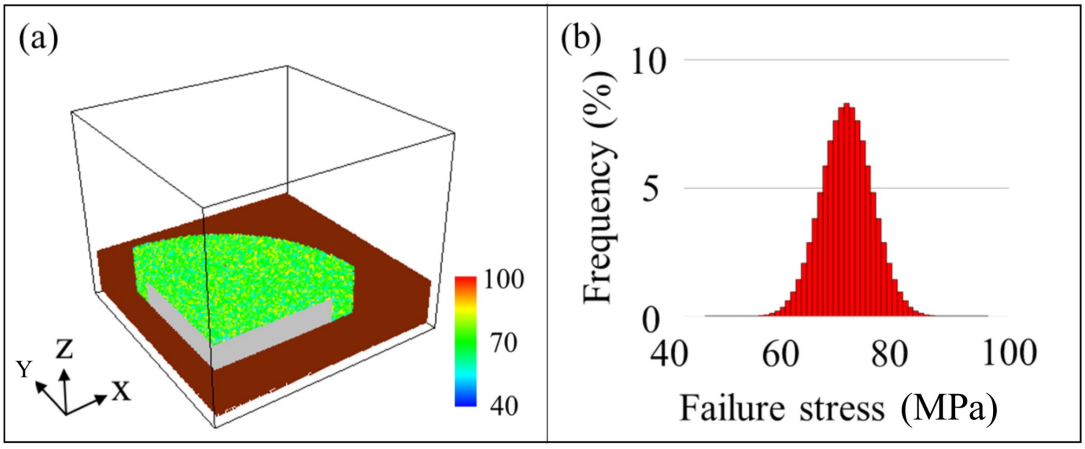


**Figure S6.** *Failure-stress distribution in the PEO SEI layer with μ = 70 MPa, σ = 7.7 MPa. (a) Failure-stress contours and (b) failure-stress histogram in the PEO layer.*

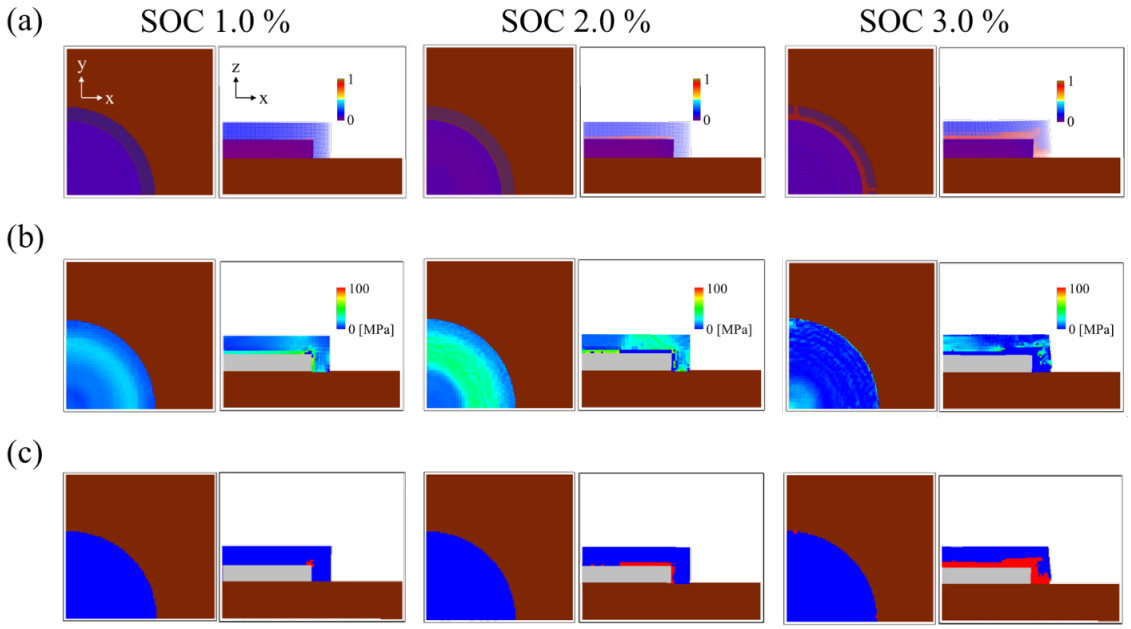


**Figure S7.** *Lithium concentration of silicon nanopillar, stress and failure evolution of the PEO SEI layer during lithiation in the brittle fracture model with stress distribution at differing SOCs.*

*Each panel displays an overhead view (left) and a side view (right). (a) lithium concentration of silicon, (b) maximum principal stress of the PEO SEI layer, and (c) failure location of the PEO SEI layer. Red and blue regions indicate the failure and non-failure regions in the SEI layer, respectively.*

*Ductile fracture model of PEO*

**Figure S8** shows the simulation results of the PEO SEI layer in the ductile fracture model. SEI failure occurred slightly inside the edge of the silicon nanopillar. The failure results resemble those in the $Li_2CO_3$ SEI layer, but appear at an earlier stage.

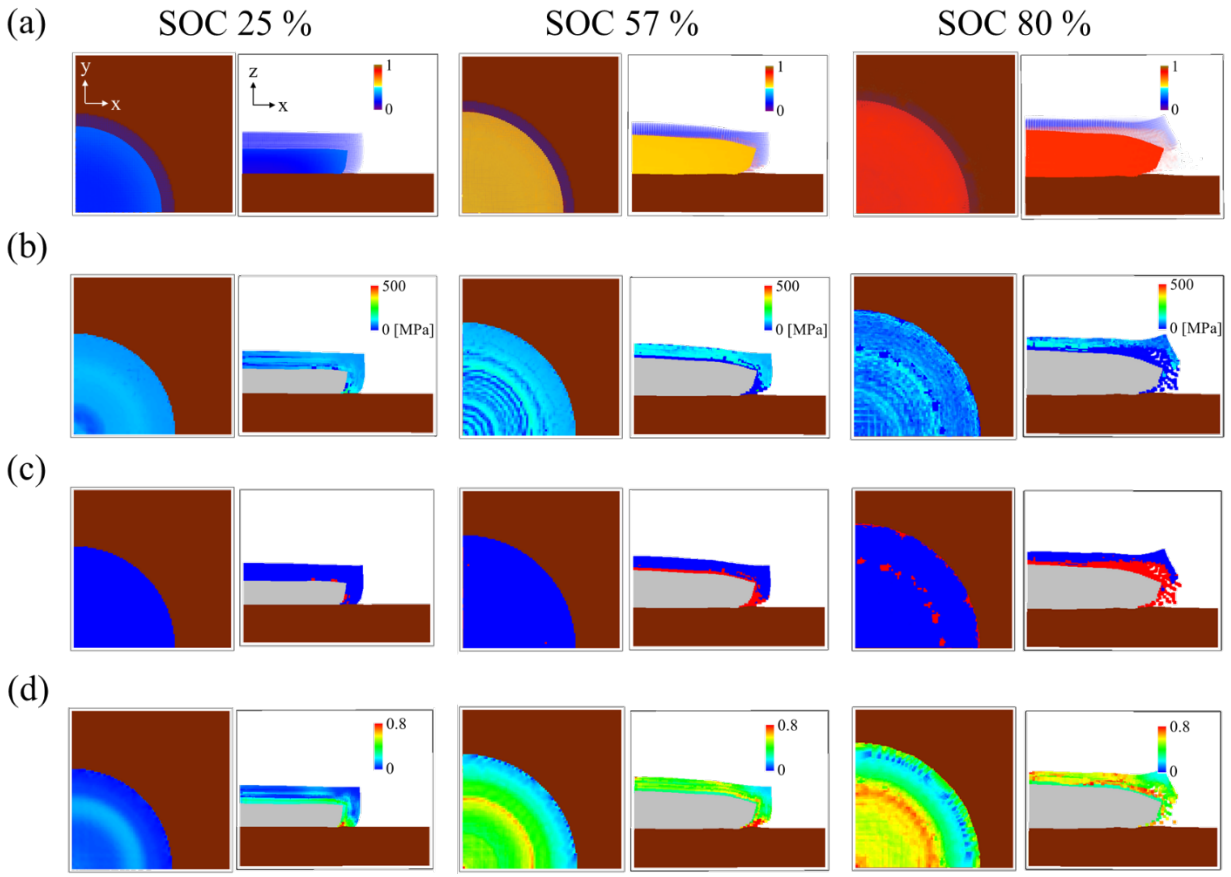


**Figure S8.** *Lithium concentration, stress, failure and plastic strain evolution of the PEO SEI layer in the ductile fracture model at differing SOCs. (a) lithium concentration of silicon, (b) effective stress of the PEO SEI layer, (c) failure location of the PEO SEI layer (Red and blue regions indicate the failure and non-failure regions in the SEI layer, respectively.) and (d) plastic strain of the PEO SEI layer.*

*The stress and the plastic strain distribution of ductile fracture model*

**Figures S9** and **S10** show the effective stress distributions and the plastic strain distributions in each SEI layer, respectively. **Tables S4** and **S5** list the values of the average and standard deviation of effective stress and plastic strain, respectively.

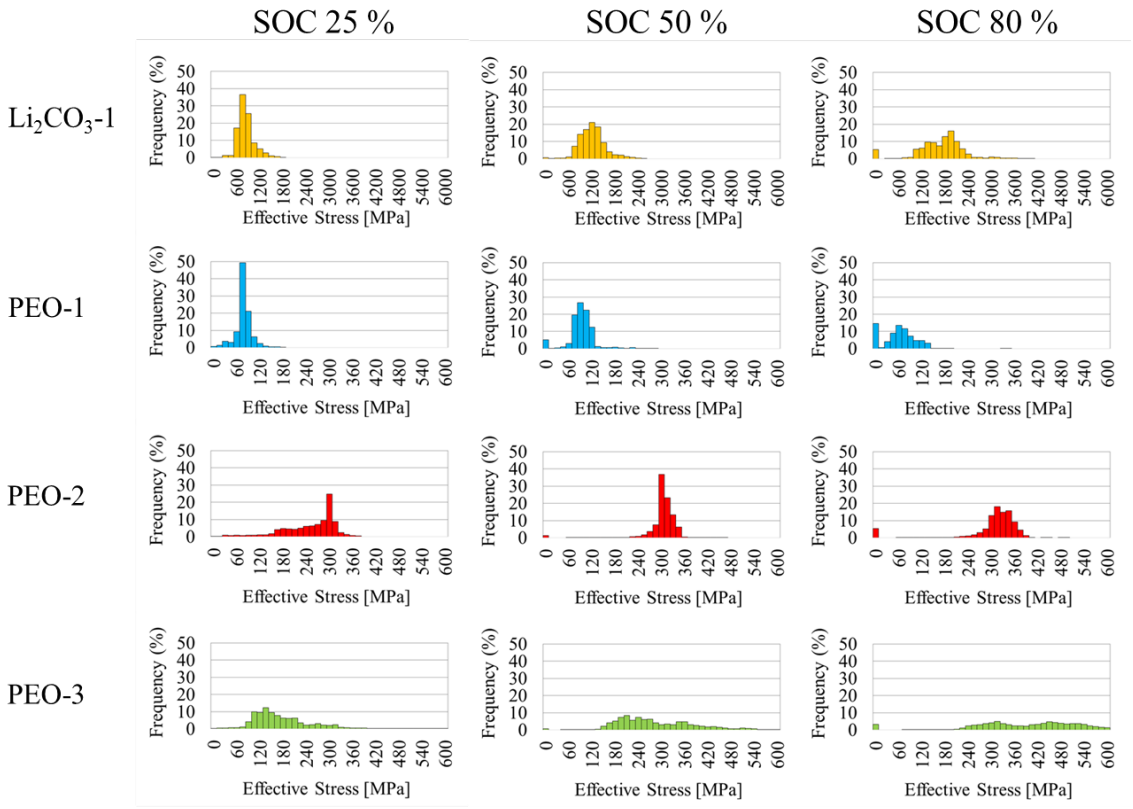


**Figure S9.** *The effective stress distributions of each SEI layer in the ductile fracture model at differing SOCs.*

**Table S4**. *Average and standard deviation values of the effective stress in each SEI layer.*

| | | SOC 25% | SOC 50% | SOC 80% |
|---|---|---|---|---|
| $Li_2CO_3$-1 | average [MPa] | 911 | 1272 | 1688 |
| | standard deviation [MPa] | 209 | 342 | 688 |
| PEO-1 | average [MPa] | 83 | 94 | 48 |
| | standard deviation [MPa] | 23 | 39 | 46 |
| PEO-2 | average [MPa] | 258 | 302 | 295 |
| | standard deviation [MPa] | 69 | 62 | 105 |
| PEO-3 | average [MPa] | 191 | 293 | 436 |
| | standard deviation [MPa] | 94 | 125 | 183 |

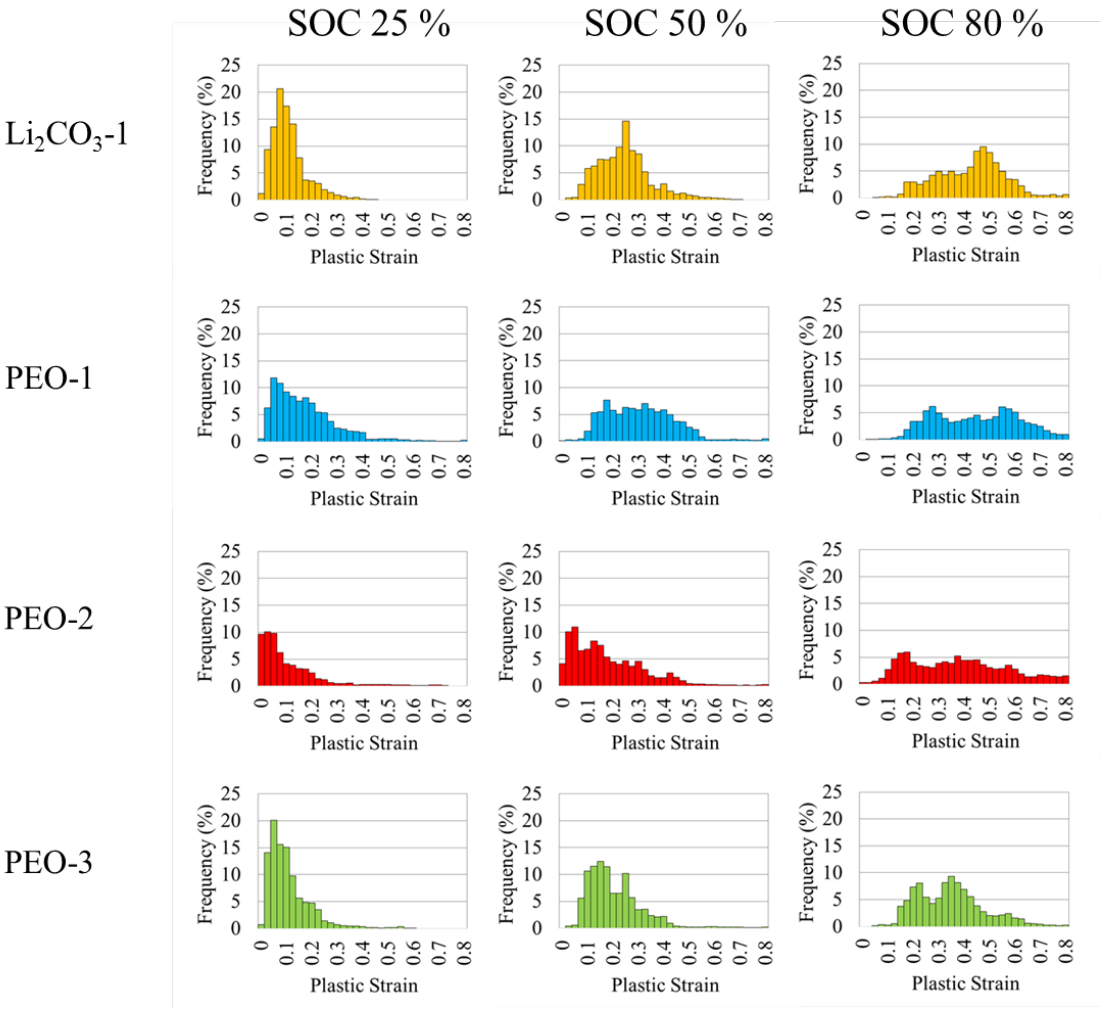


**Figure S10.** *The plastic strain distributions of each SEI layer in the ductile fracture model at differing SOCs.*

**Table S5**. *Average and standard deviation values of plastic strain in each SEI layer.*

| | | SOC 25% | SOC 50% | SOC 80% |
|---|---|---|---|---|
| $Li_2CO_3$-1 | average | 0.12 | 0.26 | 0.45 |
| | standard deviation | 0.07 | 0.10 | 0.16 |
| PEO-1 | average | 0.19 | 0.35 | 0.51 |
| | standard deviation | 0.14 | 0.21 | 0.26 |
| PEO-2 | average | 0.07 | 0.20 | 0.40 |
| | standard deviation | 0.11 | 0.18 | 0.22 |
| PEO-3 | average | 0.12 | 0.22 | 0.37 |
| | standard deviation | 0.08 | 0.12 | 0.15 |

*Effect of silicon geometry*

To examine the failure evolution in the PEO SEI layer (PEO-1) under conditions that better replicate the experimental observations, we simulated the MPM in a rectangular parallelepiped geometry.[14] The silicon was surface-coated with a 300-nm SEI. The sides and height of the silicon layer were 2.5 μm and 200 nm, respectively. The substrate was sized 3.5 μm × 3.5 μm × 100 nm. The dimensions of each grid cell were 100 nm × 100 nm × 100 nm. The system is schematized in **Figure S11**.

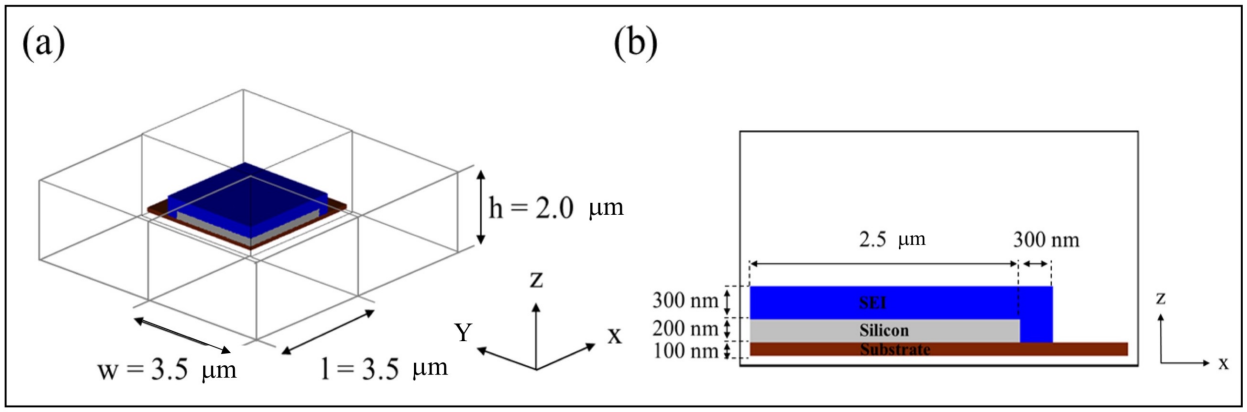


**Figure S11.** *Schematic illustration and dimensions of the MPM in the rectangular parallelepiped geometry: (a) a quarter of the actual (axially symmetric) domain simulated in the MPM; (b) side view of the system.*

The simulation results of the rectangular parallelepiped model are shown in **Figure S12**. SEI failure occurred near the corner and slightly inside the edge of the silicon nanopillar, consistent with previous experimental observations.

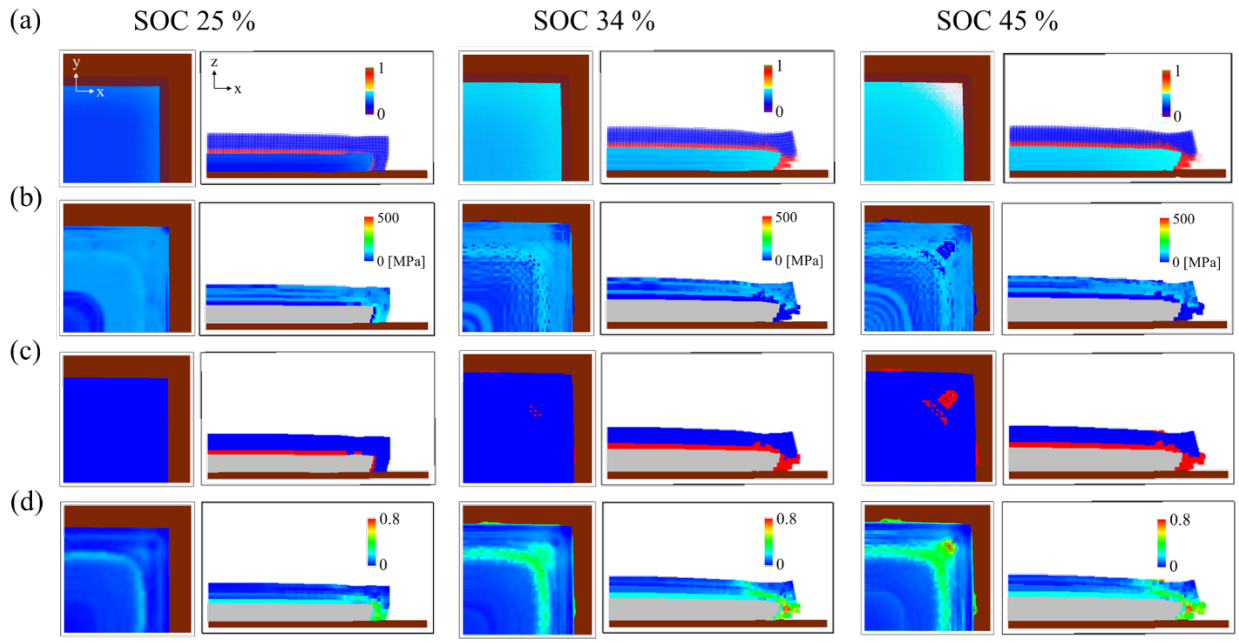


**Figure S12.** *Lithium concentration, stress, failure and plastic strain evolution of the PEO SEI layer in the ductile fracture model, constructed in the rectangular parallelepiped geometry at differing SOCs. (a) lithium concentration of silicon, (b) effective stress of the PEO SEI layer, (c) failure location of the PEO SEI layer (Red and blue regions indicate the failure and non-failure regions in the SEI layer, respectively.) and (d) plastic strain of the PEO SEI layer.*